Classification

Biological Science, Biochemistry

Title

Time-of-day dependent responses of cyanobacterial cellular viability against oxidative stress

Authors

Kenya Tanaka[1], *and Shuji Nakanishi*[1,2,*]

Author affiliation

Kenya Tanaka, [1] Graduate School of Engineering Science, Osaka University, 1-3 Machikaneyama, Toyonaka, Osaka 560-8631, Japan, tanaka@rcsec.chem.es.osaka-u.ac.jp

Shuji Nakanishi, Dr., Prof., [1] Graduate School of Engineering Science, Osaka University, 1-3 Machikaneyama, Toyonaka, Osaka 560-8631, Japan, and [2] Research Center for Solar Energy Chemistry, Osaka University, 1-3 Machikaneyama, Toyonaka, Osaka 560-8631, Japan, nakanishi@chem.es.osaka-u.ac.jp, ORICD: 0000-0002-3313-2689

Corresponding author

Shuji Nakanishi

Tel: +81-6-6850-6695, e-mail address: nakanishi@chem.es.osaka-u.ac.jp

Keywords

Circadian clock, Reactive oxygen species, Cyanobacteria, Photosynthesis

Abstract

As an adaptation to periodic fluctuations of environmental light, photosynthetic organisms have evolved a circadian clock. The gene expression of ROS scavenging enzymes is regulated by circadian clock genes, which has been considered to help deal with the diurnal photogeneration of reactive oxygen species (ROS). Although a series of recent discoveries have suggested the correlation between circadian clock control and ROS scavenging mechanisms, circadian rhythms of ROS stress tolerance have not been experimentally demonstrated to date. In the present work, we constructed a novel assay using methyl viologen (MV) which generates ROS under light irradiation and experimentally verified the circadian rhythms of ROS stress tolerance in photosynthetic cells of cyanobacterium *Synechococcus elongatus* PCC7942, a standard model species for the investigation of circadian clock. Here, we report that ROS generated by MV treatment causes damage to stroma components and not to the photosynthetic electron transportation chain, leading to reduced cell viability. The degree of decrease in cell viability was dependent on the subjective time at which ROS stress was applied. Thus, ROS stress tolerance was shown to exhibit circadian rhythms. Notably, rhythms of ROS stress tolerance disappeared in mutant cells lacking the essential clock genes. Further, ROS stress tolerance showed irregular behaviors under irregular light/dark cycles that mismatched the subjective time. These results clearly show that the antioxidant ability in the stroma varies periodically under the control of clock genes. This is the first demonstration of ROS stress tolerance in cyanobacterial cells at a phenotypic level showing circadian oscillation.

Significance statement

Reactive oxygen species (ROS) in photosynthetic organisms are the molecular basis of oxidative stress and are photogenerated in synchrony with the daily light cycles. Recent studies have revealed crosstalk between ROS scavenging systems and circadian clocks in organisms, but their mutual influence on physiological activities in a cell has not been fully elucidated. Here, we demonstrate for the first time that cellular viability against the ROS stress (i.e., ROS stress tolerance) exhibits circadian rhythms that are under the control of a clock system for cyanobacterium *Synechococcus elongatus* PCC7942, a standard model species for the investigation of the circadian clock.

Text

Oxygenic photosynthetic organisms are inescapably exposed to harmful reactive oxygen species (ROS), including singlet oxygen, superoxide anion, hydrogen peroxide, and hydroxyl radical in return for using water as an electron donor. When energy absorbed by the photosynthetic system exceeds the rate of CO_2 assimilation, ROS is abundantly produced, making timely management of ROS levels essential. ROS levels in photosynthetic organisms can be controlled by avoiding excess production of ROS through mechanisms such as cyclic electron flow, non-photochemical quenching, and the water-water cycle (1-3) or scavenging ROS that are inevitably generated. For example, superoxide dismutase and catalase are universally distributed across species and can detoxify superoxide and hydrogen peroxide, respectively. Further, ROS can be non-enzymatically reduced by lipophilic small molecules such as α-tocopherol, β-carotene, and plastoquinone (4, 5).

While changes in the light environment can be unpredictable due to various factors, all photosynthetic organisms have evolved circadian clocks to adapt to the 24 h predictable changes in light levels. Daily fluctuations in environmental light levels lead to periodic variations in ROS levels and there is thus a close correlation between the circadian clock and ROS levels and/or ROS scavenging systems (6). In fact, the expression levels of clock genes are known to be affected by ROS levels (7). Importantly, clock genes can in turn regulate the expression levels of antioxidant enzymes, providing a feedback loop between ROS level and the transcription and translation of clock genes. Moreover, it was recently reported that the redox state of peroxiredoxin, which has a primary role of H_2O_2 detoxification, exhibits a circadian rhythm independent of its transcription and translation (8, 9).

Although the relationship between the circadian clock and ROS elimination ability has been described, the impact of circadian-controlled ROS scavenging systems on physiological phenotypes has not been fully elucidated. In fact, no phenotype showing circadian rhythm in ROS stress tolerance has been experimentally confirmed to date. Thus, despite recent renewed interest in the interaction between the circadian clock and ROS stress tolerance, our current understanding on the interaction is very limited. Cyanobacterium *Synechococcus elongatus* PCC7942 (hereafter, *S. elongatus*), a photosynthetic autotrophic bacterium, is an appropriate model species for investigating these interactions because the molecular mechanism underlying its circadian clock is well understood, as summarized in recent reviews (10, 11). Here, we developed an assay to examine the effect of ROS stress on cell viability in an attempt to characterize the circadian rhythm of ROS stress tolerance.

Results

ROS generation method. In photosynthetic living cells, generation of large amounts of ROS is triggered by unfavorable conditions such as strong light irradiation or high (or low) temperature

exposure. However, these intense stimuli may mask the circadian control of ROS stress tolerance because they directly affect various metabolic pathways and induce adaptation mechanisms against ROS stress, such as structural optimization and modification of light-energy conversion systems. Lacking the detailed mechanism of ROS generation in harsh conditions might hinder understanding ROS stress tolerance. Therefore, we developed an assay using methyl viologen (MV) with light irradiation as a ROS generation system with the aim of evaluating circadian clock involvement in ROS stress tolerance control at the phenotype level.

The molecular mechanism of ROS generation by MV has been well clarified and is well suited for the present work. Specifically, MV mediates an electron transfer reaction from photosystem I (PSI) or ferredoxin to oxygen under light irradiation, resulting in the production of superoxide (12, 13). The generated superoxide is converted to H_2O_2 and hydroxyl radical by subsequent disproportionation reaction and Fenton type reaction (14). In our study, *S. elongatus* cells grown in a turbidostat were assayed for evaluation of ROS stress tolerance using the following protocol. First, 50 μM MV was added to cell culture aliquots taken at various subjective times, followed by 30 min light irradiation (This protocol for ROS generation is hereafter denoted as "MV/Light-treatment"). After the MV/Light-treatment, cells were washed with BG-11 medium and oxidative damage was evaluated by measuring oxygen evolution activity, P700 absorbance change or colony forming unit (CFU) (Fig. 1). As the addition of MV barely affects the rate of NADPH formation because of slow photosynthetic electron donation to MV compared to the flux of linear electron flow in cyanobacteria species (15), the direct influence of MV on metabolism can be neglected. ROS generation by the MV/light treatment was confirmed by assay using 2',7'-dichlorodihydrofluorescein diacetate (H_2DCFDA), which is converted by intracellular esterases to 2',7'-dichlorodihydrofluorescein, which can subsequently be oxidized by ROS to a fluorescent compound with an emission peak at around 520 nm. Thus, intracellular ROS level can be quantified by fluorescence intensity (Fig. 2). The difference in fluorescence intensity normalized by control samples incubated without MV in darkness showed light intensity dependence. A small increase in ROS level was observed even for samples incubated in darkness with 50 μM MV due to the reduction of MV by intracellular NADPH.

Effect of ROS stress on photosynthetic activity. The effects of ROS generated by the MV/light treatment on the activities of overall electron transfer including photosystem II (PSII) and photosystem I (PSI) were investigated. Overall electron transfer activity was evaluated by measuring oxygen evolution reaction (OER) rate when CO_2 ($NaHCO_3$) was used as the sole electron acceptor. The ratio of the OER rate for the cells incubated with MV against that for the cells incubated without MV shown in Fig. 3A indicates that OER rate was markedly decreased by the addition of MV for the dark condition and even more so for higher light intensity conditions. These patterns are consistent

with normalized fluorescence data in Fig. 2 showing a marked increase in ROS level by the addition of MV even in dark and light intensity dependence. Notably, the difference in OER rate was not significantly different for incubation with MV at 10 and 100 μmol $m^{-2}s^{-1}$), suggesting that damage to the photosynthetic systems of samples with MV reached a maximum at light intensity 10 μmol $m^{-2}s^{-1}$.

Next, PSII activity was evaluated by measuring OER rate in the presence of 2,6-dichlorobenzoquinone (DCBQ), which intercepts photosynthetic electrons from PSII. The OER rate was not affected by the addition of MV or light intensity (Fig. 3B) while it was affected when CO_2 was used as the electron acceptor (Fig. 3A). This was either because ROS generated by MV addition did not damage PSII or any damaged PSII was quickly repaired. To verify which pathway was producing the observed result, PSII activity measurements were performed in the presence of a translation inhibitor, chloramphenicol (Cm), which prevents repair of PSII. Cells incubated in a medium containing Cm but no MV showed reduced PSII activity when exposed to light at an intensity of 100 μmol $m^{-2}s^{-1}$ (Fig. S1). However, PSII activity at a light intensity of 10 μmol $m^{-2}s^{-1}$ in the presence of Cm was maintained at the same level as that in the absence of Cm, indicating that photoinhibition of PSII does not occur under irradiation of 10 μmol $m^{-2}s^{-1}$. On the other hand, MV/light treatment did not affect PSII activity irrespective of light intensity (Fig. 3B). These results indicate that ROS generated under MV/light treatment does not damage PSII.

Oxidative damage to PSI was also evaluated using an established protocol based on the absorption spectroscopy for the reaction center of PSI (chlorophyll, P700) (15). As shown in Fig. 3C, the amount of oxidizable P700 (Pm) in cells treated with MV was constant over the range of light intensity tested, indicating that MV/light treatment did not damage PSI.

Finally, the effect of ROS on the photosynthetic electron transport chain (PETC), including all components from PSII to PSI, was tested by measuring light-induced O_2 uptake rate with H_2O and MV serving as the electron donor and accepter, respectively. As shown in Fig. 3D, cells treated by the MV/light treatment maintained electron transfer activity at the same level for light irradiation at 10 and 100 μmol $m^{-2}s^{-1}$. Taken together, generated ROS did not damage PETC which is itself the machinery for generating ROS.

Effect of ROS stress on cell viability. Next, we examined the influence of MV/light treatment on cell viability. Treated cells were cultured on agar plates, and the number of colonies after 6 or 7 days was counted (Fig. 3E). Although ROS levels increased and photosynthetic activity decreased when cells were incubated in darkness with MV, as shown in Figs. 2, 3A, there were no significant differences in the colony-forming unit (CFU) between samples incubated in weak light irradiation without MV and darkness with MV. Contrary to this, CFU values of the MV/light treated cells decreased in a light intensity-dependent manner, indicating that ROS generated from PETC through

MV reduced cell viability. In addition, the result that CFU changed depending on light intensity during MV/light treatment means that the CFU was not influenced by residual MV during culturing on agar plates.

Oxidative damage to PSII or PSI is known to be caused by ROS generation due to excessive reduction of PETC components but not by ROS generation due to external addition of H_2O_2 or MV (16-18). In good agreement with these studies, as mentioned earlier, PETC activity was not impacted by oxidative stress induced by the MV/light treatment. On the other hand, overall photosynthetic activity and CFU values were decreased by MV/light-treatment (Figs. 3A, E). These results clearly indicate that stromal components, including enzymes participating in electron flux downstream of PSI, were damaged by ROS. In fact, lipids, DNA and Rubisco with CO_2 fixing ability are known to be damaged by ROS generated by MV (19, 20). Oxidative damage to such components is likely to have caused a decrease in overall electron transfer activity and CFU.

Effect of the circadian clock on ROS stress tolerance. Oxidative stress was applied to cells sampled at various subjective times using the MV/light treatment to investigate circadian control of ROS stress tolerance. For these tests, cells cultured in the turbidostat with cell density kept constant (optical density 730 nm (OD_{730}) = 0.6 ± 0.1, Fig. S2) were used to exclude the possibility that differences in growth stage influence the CFU results in experiments. Light intensity during the MV/light treatment was set to 10 μmol $m^{-2}s^{-1}$ to avoid photoinhibition of PSII (Fig. S1). After subjecting the cells to light-dark (LD) cycles with 24 h periodicity, cells were exposed to a continuous light (LL) condition (Figs 4A and S3). While non-treated wild type (WT) cells (filled circles) showed no dependence on subjective time, MV/light treated cells showed circadian rhythm (open circles). Mutant cells lacking clock genes (*ΔkaiABC*) did not show clear rhythms regardless of whether they were MV/light treated or not (closed and open squares in Fig. 4A). Importantly, the oscillatory phase of the ROS stress tolerance rhythm was determined by phase of LD cycles (Fig. 4B). Further, using period mutant cells (F470Y, S157P) having a free running period (FRP) of 16 and 21 h, respectively (21), CFU results showed periodicity corresponding with the FRP (Fig. 5). Although these results suggest that KaiABC controls ROS stress tolerance of a cell, there is a possibility that circadian rhythms in CFU can be induced by rhythmical change in the amount of ROS generated by the MV/light treatment. However, electron flux in PETC where ROS is generated is known to be constant in the LL condition in *S. elongatus* (22,23). Further, as shown above, PETC itself was shown to not be damaged by the MV/light treatment. Thus, it can be concluded that the difference in the amount of generated ROS at various subjective times is negligible.

Next, we examined the temporal change in ROS stress tolerance using cells that had been exposed to varying light-dark schedules. In LL conditions, CFU time series data showed maximum values at subjective dawn and the lowest values at the subjective dusk (Figs. 4, 6A). On the other

hand, in LD conditions, bimodal CFU time courses with peaks around 4 and 16 h of Zeitgeber time were observed (Fig. 6B). In *S. elongatus*, glycogen accumulation is programmed to be activated to coincide with reduced cell division rate at the subjective dusk by the circadian clock system (24-26). Supply of reducing power through catabolism of accumulated glycogen could keep the intracellular ROS levels low, even in the dark, when reducing power is not generated by photosynthesis (27). In good agreement with these studies, the increase in ROS stress tolerance was observed in the first half of the dark period. It is likely that the decrease in ROS stress tolerance in the latter half of the dark period is due to a deficiency in the amount of stored glycogen in a cell (24) and/or due to a distribution of stored energy to cell division rate increase (25). This explanation can be rationalized by the fact that a bimodal rhythm was not observed in the LL condition when reducing power can be generated at all times throughout photosynthesis (Figs. 4, 6A).

When a 12 h dark pulse was applied at the subjective daytime to disturb the circadian rhythms, CFU values began to decrease as early as 4 h after onset of the dark pulse (Fig. 6C). Comparing Figs. 6B and C shows that the increase in the CFU values during the dark period was observed only in cells that were synchronized in the regular 24 h LD cycle. These results indicate that the characteristic time profiles of CFU values under LD conditions reflect the ROS stress tolerance controlled by the circadian clock system.

Discussion. As shown in our study, ROS stress tolerance rhythms were observed in cell viability (Fig. 4, 6A). Considering that the MV/light treatment causes damage to stromal components, it can be concluded that ROS scavenging ability (i.e., antioxidant ability) in the stroma varied rhythmically. How could periodic changes in ROS scavenging ability occur? In general, antioxidant enzymes and reducing power are required for detoxifying ROS. Therefore, observation of circadian rhythm in ROS stress tolerance indicates that the amount of antioxidant enzymes and/or intracellular reducing power changes over a day under the control of a circadian clock system. Microarray analyses of *S. elongatus* cells have revealed that various mRNA expression levels, including superoxide dismutase and peroxiredoxins exhibited circadian rhythms (28). However, much fewer numbers of proteins exhibited daily rhythms in the LD condition, and more importantly, no known antioxidant enzymes were included in proteins groups that exhibit rhythmic expression (29). Therefore, contribution of diurnal variation of expression level of antioxidant enzymes to ROS stress tolerance rhythms may be limited. In contrast, a clear circadian rhythm in reducing power has been demonstrated; for example, in electrochemically demonstrated intracellular redox rhythms (23, 30). Further, as mentioned earlier, NADPH production was shown to be activated at night based on glycogen accumulated in the subjective dusk (25). In other words, NADPH generation, hence the intracellular redox, is periodically activated under control of the circadian clock.

Altogether the present study demonstrated circadian clock control of ROS stress tolerance

changes in *S. elongatus*. Although the addition of 50 µM MV is known to cause an adaptive response that increases mRNA accumulation of peroxiredoxins within 30 min (31), cell viability periodically changed in a subjective time-dependent manner, indicating that pre-adaptation against ROS stress through the circadian clock system was more efficiently achieved through post-adaptive responses. Further study along these lines will deepen our understanding of competitive fitness advantages, as well as the origin and evolution of the circadian clock (9, 10).

Materials and Methods

Bacterial strains and cell culture conditions. We used the following *S. elongatus* strains: wild-type reporter strains (P_{kaiBC}*::luxAB* and P_{psbAI}*::luxCDE*) (32), *kaiABC*-deficient P_{kaiBC} reporter strain (33) and two *kaiC* mutant strains with short periodicity carrying P_{kaiBC} reporters (F470Y and S157P) (21). These strains were grown in liquid or on solid (1.5% Bacto agar) BG-11 medium. Liquid cultures were grown in flasks (batch culture) or turbidostat (continuous culture) at 30 ºC with air bubbling and exposure to light at an intensity of 30-40 µmol $m^{-2}s^{-1}$. For continuous culture, cell density was continuously monitored using an optical sensor with near-infrared light (NI; 840 nm ~ 910 nm), and cell density was controlled by dilution with fresh medium when the OD value in the NI region exceeded a certain value.

Methyl viologen (MV) treatment. MV was added at a final concentration of 50 µM to liquid culture medium to achieve optical density at 730 nm (OD_{730}) of 0.65±0.05. Negative control samples without MV were prepared at the same time. The samples were incubated for 30 min at the specified light intensity, and cells were collected by 5-min centrifugation at 4,400 xg at 30 ºC, re-suspended in fresh BG-11 medium to remove MV, centrifuged again, and re-suspended again in fresh BG-11 to produce the cell density required for subsequent measurements.

Measurement of intracellular ROS level. Intracellular ROS level was measured as described previously with slight modifications (27, 34). H_2DCFDA (Invitrogen) was dissolved in ethanol to produce a 15 mM stock solution just before the assay. H_2DCFDA stock solution or ethanol (vehicle) was added to liquid culture with OD_{730} of 0.65±0.05, and the solution was incubated in darkness for 30 min at 30 ºC. Then, H_2DCFDA was removed from culture medium by centrifugation, and culture medium was combined with an equal amount of fresh BG-11 medium, and 50 µM MV was or was not added. The cell suspension was incubated for 30 min at the indicated light intensity at 30 ºC to generate ROS. The treated cells were placed in a 96-well plate, and fluorescence emission at 535 nm was measured with excitation at 485 nm on a Tecan Infinite M200 Plate Reader. Background fluorescence signal of the samples without H_2DCFDA (ethanol only) was subtracted from the fluorescence values of the corresponding samples with H_2DCFDA.

Measurement of oxygen concentration. Reaction mixtures containing BG-11 with 40 mM TES-NaOH (pH 7.5), 50 mM $NaHCO_3$ and cells after MV treatment (10 µg Chl/mL) were stirred with a magnetic stirrer, and the oxygen concentration was monitored using an oxygen electrode (Hansatech, UK). Overall activity was determined by light irradiation with an LED source (pE-100^{wht}, BioVision Technologies, USA) through 550 nm long pass filter at light intensity of 660 µmol $m^{-2}s^{-1}$. Then, 0.4 mM 2,6-dichlorobenzoquinone (DCBQ) was added to determine PSII activity. To determine electron transfer activity from PSII to PSI, light-induced oxygen uptake of MV-treated cells was measured in the presence of 1 mM KCN, 1 mM MV, and 10 mM methyl amine.

Photochemical measurement of total P700. Absorbance changes of P700 (reaction center chlorophyll of PSI) were monitored using a fiber version of Dual-PAM-100 at room temperature. Samples containing BG-11 with 40 mM TES-NaOH (pH 7.5) and cells after the MV treatment (15 µg Chl /mL) were introduced to a cuvette. To measure maximum P700 absorption, saturating pulse illumination (10,000 µmol $m^{-2}s^{-1}$) was applied after irradiation with blue light (750 µmol $m^{-2}s^{-1}$) for 5 s.

Viable cell plating. Samples after MV treatment were re-suspended in fresh BG-11 to reach OD_{730} of 0.3. Each sample was serially diluted 1:10 four times in fresh BG-11 and then 4 µL of each dilution was spotted onto solid BG-11 plates without antibiotics. The plates were incubated at 30 ºC under 30 µmol $m^{-2}s^{-1}$ constant light for 6 or 7 days and then photographed.

Acknowledgments. We thank Prof. K. Terauchi (Ritsumeikan University) and Prof. T. Kondo (Nagoya University) for kindly providing the mutant strains used in this work; Prof. K. Tanaka and Mr. T. Tsurumaki (Tokyo Institute of Technology) for providing us the key suggestion regarding the clock-controlled ROS tolerance through a presentation at the 59th Annual Meeting of the Japanese Society of Plant Physiologists (Sapporo, Japan 2018); Dr. G. Shimakawa for sharing advice and opinions about oxygen concentration and P700 absorption measurement. This work was partially supported by the Advanced Low Carbon Technology Research and Development Program (JPMJAL1402) of the Japan Science and Technology Agency (JST) and JSPS KAKENHI Grant Number 18J20176.

References

1. Munekage Y, et al. (2004) Cyclic electron flow around photosystem I is essential for photosynthesis. *Nature* 429:579-582.
2. Jahns P, Holzwarth AR (2012) The role of the xanthophyll cycle and of lutein in photoprotection

of photosystem II. *Biochim Biophys Acta* 1817:182–193.

3. Asada K, (1999) The water-water cycle in chloroplasts: Scavenging of active oxygens and dissipation of excess photons. *Annu Rev Plant Physiol Plant Mol Biol* 50:601-639.
4. Kruk J, Szymanska R, Nowicka B, Dłuzewska J (2016) Function of isoprenoid quinones and chromanols during oxidative stress in plants. *N Biotechnol* 33:636–643.
5. Ramel F, et al. (2012) Chemical quenching of singlet oxygen by carotenoids in Plants. *Plant Physiol* 158:1267–1278.
6. Stangherlin A, Reddy AB (2013) Regulation of circadian clocks by redox homeostasis. *J Biol Chem* 288:26505–26511.
7. Grace A, et al. (2012) *CIRCADIAN CLOCK-ASSOCIATED* 1 regulates ROS homeostasis and oxidative stress responses. *Proc Natl Acad Sci USA* 109:17129–17134.
8. O'Neill J, Reddy A (2011) Circadian clocks in human red blood cells. *Nature* 469:498–503.
9. Edgar RS, et al. (2012) Peroxiredoxins are conserved markers of circadian rhythms. *Nature* 485:459–464.
10. Johnson CH, Zhao C, Xu Y, Mori T (2017) Timing the day: what makes bacterial clocks tick? *Nat Rev Microbiol* 15:232-242.
11. Swan JA, Golden SS, LiWang A, Partch CL (2018) Structure, function, and mechanism of the core circadian clock in cyanobacteria. *J Biol Chem* 293:5026-5034.
12. Farrington JA, Ebert M, Land EJ, Fletcher K (1973) Bipyridylium quaternary salts and related compounds. V. Pulse radiolysis studies of the reaction of paraquat radical with oxygen. Implications for the mode of action of bipyridyl herbicides. *Biochim Biophys Acta* 314:372-381.
13. Sétif P (2015) Electron-transfer kinetics in cyanobacterial cells: methyl viologen is a poor inhibitor of linear electron flow. *Biochim Biophys Acta* 1847:212-222.
14. Babbs CF, Pham JA, Coolbaugh RC (1989) Lethal hydroxyl radical production in paraquat-treated plants. *Plant Physiol* 90:1267-1270.
15. Christof K, Ulrich S (1994) An improved method, using saturating light pulses, for the determination of photosystem I quantum yield via$P700^+$-absorbance changes at 830 nm. *Planta* 192:261-268.
16. Herbert SK, Samson G, Fork DC, Laudenbach DE (1992) Characterization of damage to photosystems I and II in a cyanobacterium lacking detectable iron superoxide dismutase activity. *Proc Natl Acad Sci USA* 89:8716-8720.
17. Sonoike K (1996) Degradation of *psaB* gene product, the reaction center subunit of photosystem I, is caused during photoinhibition of photosystem I: possible involvement of active oxygen species. *Plant Sci* 115:157-164.
18. Allakhverdiev SI, Murata N (2004) Environmental stress inhibits the synthesis de novo of proteins involved in the photodamage-repair cycle of Photosystem II in *Synechocystis* sp. PCC

6803. *Biochim Biophys Acta* 1657:23-32.

19. Desimone M, Henke A, Wagner E (1996) Oxidative Stress Induces Partial Degradation of the Large Subunit of Ribulose-1,5-Bisphosphate Carboxylase/Oxygenase in Isolated Chloroplasts of Barley. *Plant Physiol* 111:789-796.
20. Imlay JA (2003) Pathways of oxidative damage. *Annu Rev Microbiol* 57:395-418.
21. Nakajima M, et al. (2005) Reconstitution of circadian oscillation of cyanobacterial KaiC phosphorylation in vitro. *Science* 308:414-415.
22. Yen U, Huang T, Yen T (2004) Observation of the circadian photosynthetic rhythm in cyanobacteria with a dissolved-oxygen meter. *Plant Sci* 166:949–952.
23. Tanaka K, Ishikawa M, Kaneko M, Kamiya K, Kato S, Nakanishi S (2019) The endogenous redox rhythm is controlled by a central circadian oscillator in cyanobacterium *Synechococcus elongatus* PCC7942. *Photosynth Res* doi: 10.1007/s11120-019-00667-0.
24. Diamond S, Jun D, Rubin BE, Golden SS (2015) The circadian oscillator in Synechococcus elongatus controls metabolite partitioning during diurnal growth. *Proc Natl Acad Sci USA* 112:E1916-E1925
25. Lambert G, Chew J, Rust MJ (2016) Costs of clock-environment misalignment in individual cyanobacterial cells. *Biophys J* 111:883–891.
26. Pattanayak GK, Phong C, Rust MJ (2014) Rhythms in energy storage control the ability of the cyanobacterial circadian clock to reset. *Curr Biol* 24:1934-1938.
27. Diamond S, et al. (2017) Redox crisis underlies conditional light–dark lethality in cyanobacterial mutants that lack the circadian regulator, RpaA. *Proc Natl Acad Sci USA* 114:E580–E589.
28. Ito H, et al. (2009) Cyanobacterial daily life with Kai-based circadian and diurnal genome-wide transcriptional control in *Synechococcus elongatus. Proc Natl Acad Sci USA* 106:14168–14173.
29. Guerreiro AC, et al. (2014) Daily rhythms in the cyanobacterium *Synechococcus elongatus* probed by high-resolution mass spectrometry-based proteomics reveals a small defined set of cyclic proteins. *Mol Cell Proteomics* 13:2042-2055.
30. Nishio K, et al. (2015) Electrochemical detection of circadian redox rhythm in cyanobacterial cells via extracellular electron transfer. *Plant Cell Physiol* 56:1053–1058.
31. Stork T, Michel KP, Pistorius EK, Dietz KJ (2005) Bioinformatic analysis of the genomes of the cyanobacteria *Synechocystis* sp. PCC 6803 and *Synechococcus elongatus* PCC 7942 for the presence of peroxiredoxins and their transcript regulation under stress. *J Exp Bot* 56: 3193-3206.
32. Lu Y, et al. (2014) Regulation of the cyanobacterial circadian clock by electrochemically controlled extracellular electron transfer. *Angew Chem Int Ed Engl* 53:2208–2211.
33. Ishiura M, et al. (1998) Expression of a Gene Cluster *kaiABC* as a Circadian Feedback Process in Cyanobacteria. *Science* 281:1519–1524.
34. Sae-Tang P, Hihara Y, Yumoto I, Orikasa Y, Okuyama H, Nishiyama Y (2016) Overexpressed

Superoxide Dismutase and Catalase Act Synergistically to Protect the Repair ofPSII during Photoinhibition in *Synechococcus elongatus* PCC 7942. *Plant Cell Physiol* 57:1899-1907.

Figures

Figure 1. Schematic of *S. elongatus* growth, followed by ROS generation with the addition of MV with light incubation (MV/light treatment) and the ROS tolerance evaluation. MV: methyl viologen, PSI: photosystem I, PSII: photosystem II.

Figure 2. Effect of addition of MV and light irradiation intensity on intracellular ROS level. Wild type cells were incubated without MV (w/o MV) or with 50 µM MV (w/ MV) under three levels of light intensity (0, 10, and 100 µmol m^{-2} s^{-1}) for 30 min. Fluorescence intensity of control samples (w/o H_2DCFDA) was subtracted from the fluorescence intensity of samples with H_2DCFDA, and the differences in fluorescence between with and without MV at each light intensity level are presented. Fluorescence intensity from three biological replicates were measured in each experiment. Values are means ± SD (bars) results from three independent experiments (therefore, each bar is the average of n = 9).

Figure 3. Evaluation of oxidative stress generated by MV/light treatment. Ratio of oxygen evolution rate of 10 µg Chl/ml suspension containing cells treated with and without 50 µM MV under three light intensities (MV/light treatment) was measured in the presence of (A) $NaHCO_3$, (B) DCBQ, or DCBQ and 200 µg/ml chloramphenicol, indicated as PSII and PSII (Cm), respectively. (C) Oxidizable P700 (Pm) and (D) Ratio of oxygen uptake rate of 10 µg Chl/ml suspension containing cells treated with and without 50 µM MV for the examination of oxidative damage due to the MV/light treatment on the photosynthetic electron transport chain, including components from PSII to PSI. For measurements of oxygen uptake, 1 mM MV, 1 mM KCN and 10 mM methyl amine were added to 10 µg Chl/ml suspension containing MV/light treated cells in an oxygen electrode chamber. (A-D) Values and error bars represent means ± SD of three independent experiments. (E) MV/light treated cells were spotted on agar plates and grown to visualize the effect of the MV/light treatment on cell viability. Obtained colonies were counted to calculate CFU. Values and error bars represent means ± SD of three biological replicates.

Figure 4. Time series of CFU of MV/light treated cells. (A) Wild type (WT) and *kaiABC*-deficient mutant (*ΔkaiABC*) cells were harvested from turbidostat every 6 h, followed by the MV/light treatment (10 µmol/(m^2 s)) to each aliquot. Oxidative stress tolerance was visualized as the number of grown colonies and (B) ROS tolerance of WT cell cultures entrained in antiphase were tested every 6 h. Luminescence rhythms of WT cells were also measured to identify phase of each culture, and shown above the CFU graph. White and black or orange bars denote light-dark (LD) cycles. Values and error bars represent means ± SD of three biological replicates.

Figure 5. Correlation of period length between gene expression rhythm and ROS tolerance rhythm of period mutant strains. ROS tolerance of (A) F470Y and (B) S157P strains cultured in continuous light condition following 12 h light/12 h dark cycles for entrainment were tested. Gray lines indicate luminescence traces of the cells to confirm short-period phenotype. Values represent means of three biological replicates.

Figure 6. Time-dependent ROS tolerance changes of cells cultured under various light-dark schedules. WT cells were cultured in a turbidostat under (A) continuous light, (B) regular 12 h light/12 h dark (LD) cycles, and (C) LD cycles mismatched to the subjective time. ROS tolerance was examined on aliquots taken from each culture. Black lines in (B) and (C) represent CFU traces of samples treated without MV. Colored lines in (B) and (C) are CFU traces of MV/light treated samples in three or two different batches of experiments for confirming repeatability. Values and error bars represent means ± SD of three biological replicates.

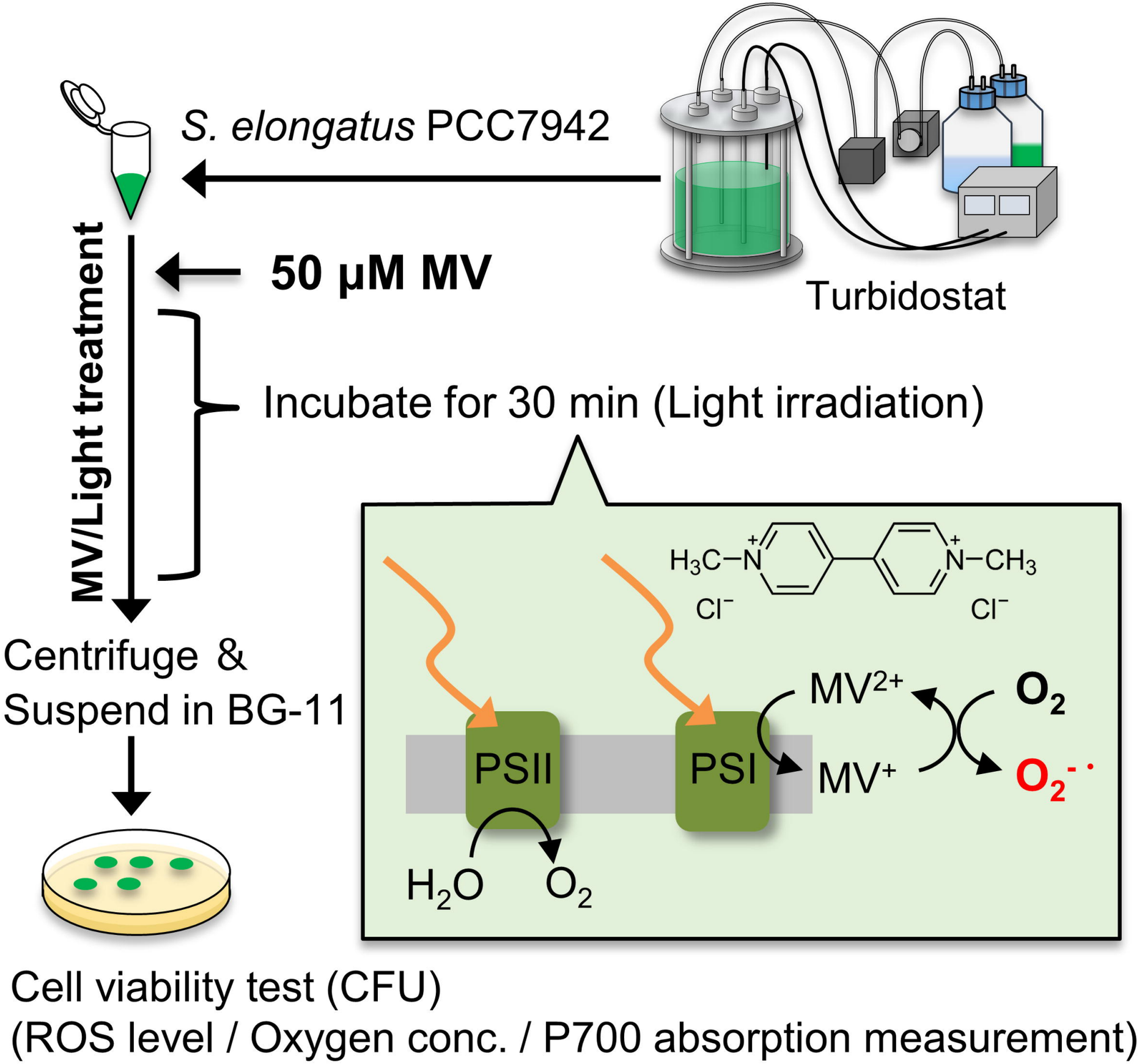
S. elongatus PCC7942
Turbidostat
50 μM MV
MV/Light treatment
Incubate for 30 min (Light irradiation)
Centrifuge &
Suspend in BG-11
PSII
PSI
H2O
O2
MV2+
MV+
O2
O2-·
Cl−
Cl−
Cell viability test (CFU)
(ROS level / Oxygen conc. / P700 absorption measurement)

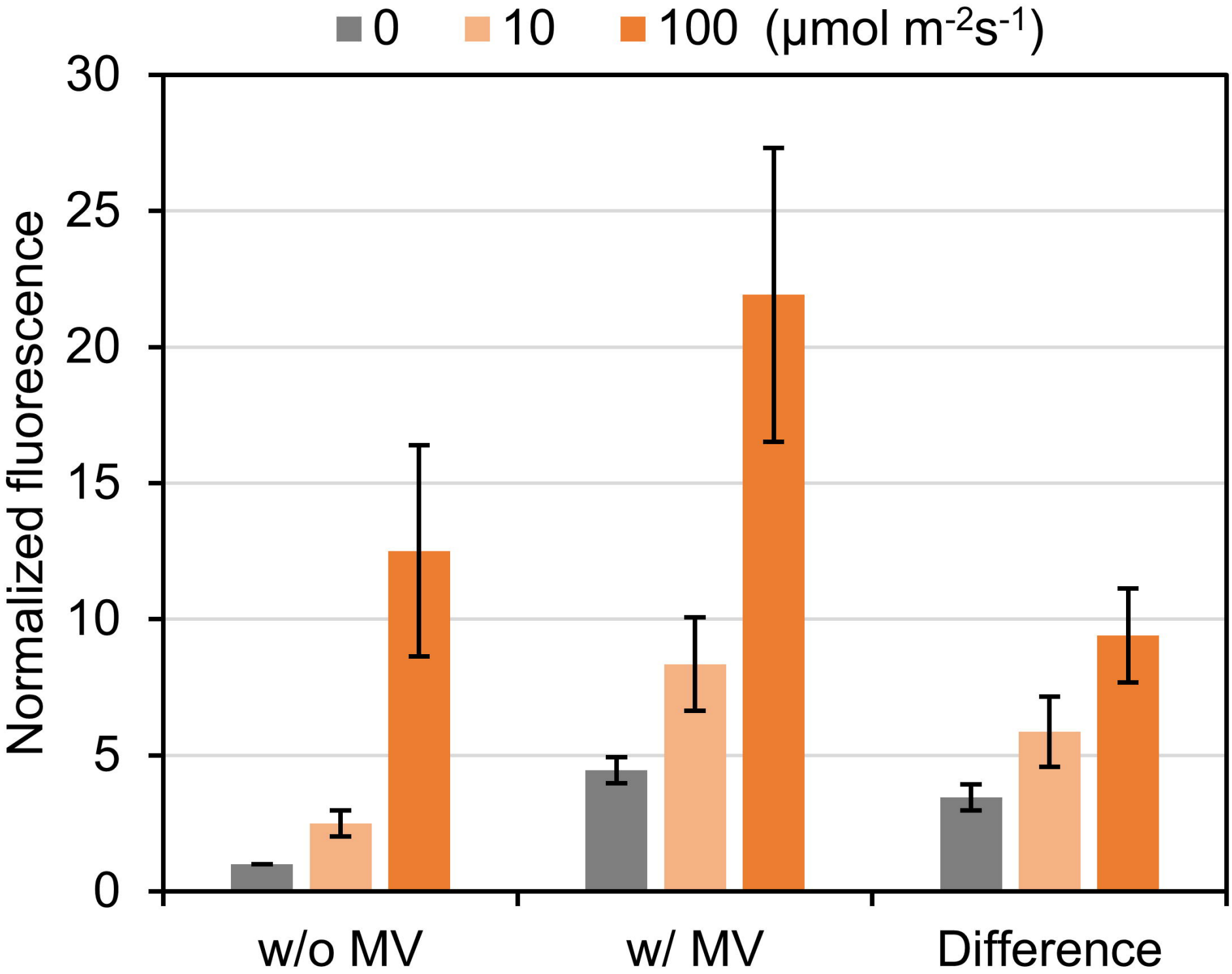
0
10
100 (μmol m-2s-1)
30
25
20
15
10
5
0
Normalized fluorescence
w/o MV
w/ MV
Difference

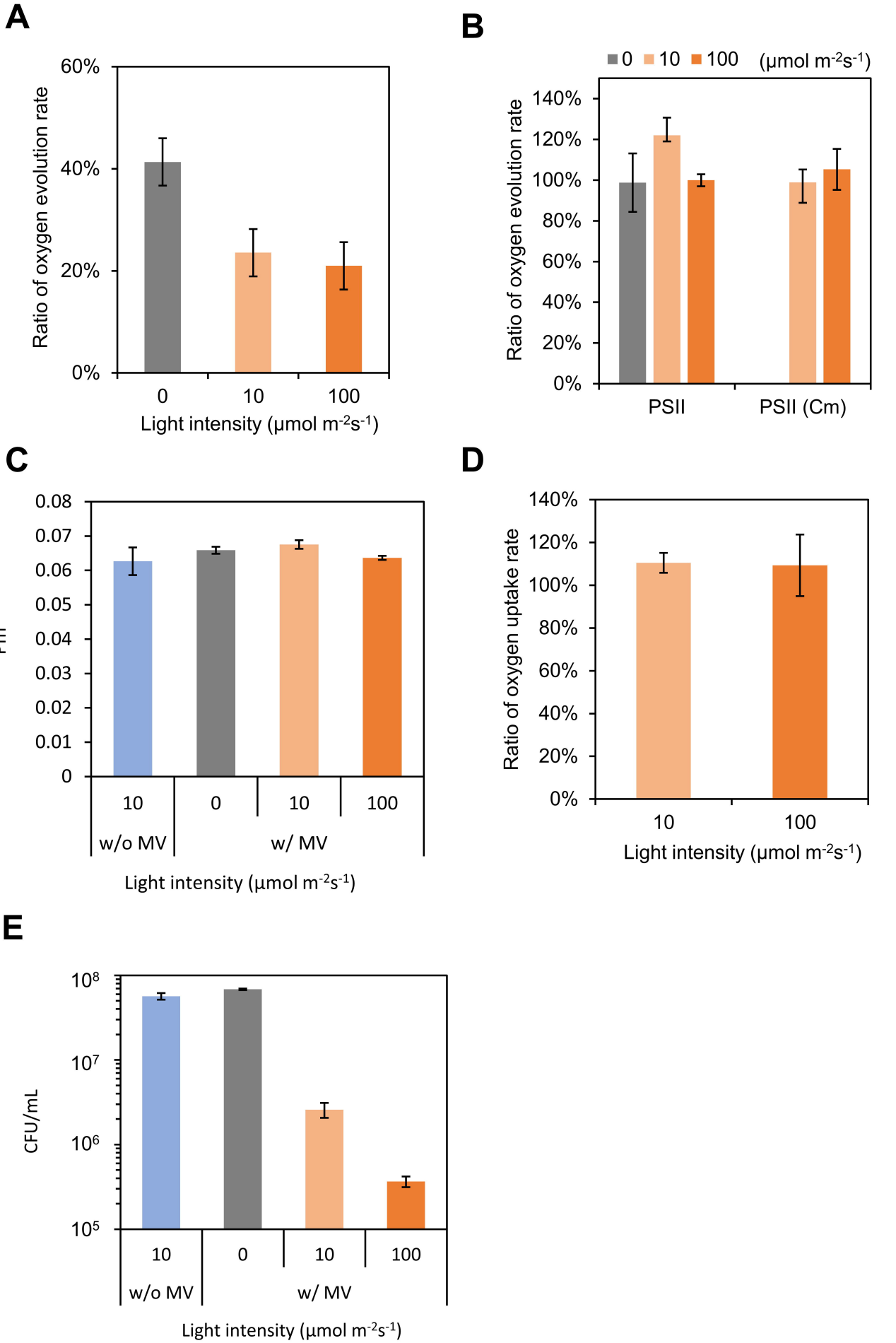
A
60%
40%
20%
0%
Ratio of oxygen evolution rate
0
10
100
Light intensity (μmol m-2s-1)
B
0
10
100
(μmol m-2s-1)
140%
120%
100%
80%
60%
40%
20%
0%
Ratio of oxygen evolution rate
PSII
PSII (Cm)
C
0.08
0.07
0.06
0.05
0.04
0.03
0.02
0.01
0
Pm
10
0
10
100
w/o MV
w/ MV
Light intensity (μmol m-2s-1)
D
140%
120%
100%
80%
60%
40%
20%
0%
Ratio of oxygen uptake rate
10
100
Light intensity (μmol m-2s-1)
E
10^8
10^7
10^6
10^5
CFU/mL
10
0
10
100
w/o MV
w/ MV
Light intensity (μmol m-2s-1)

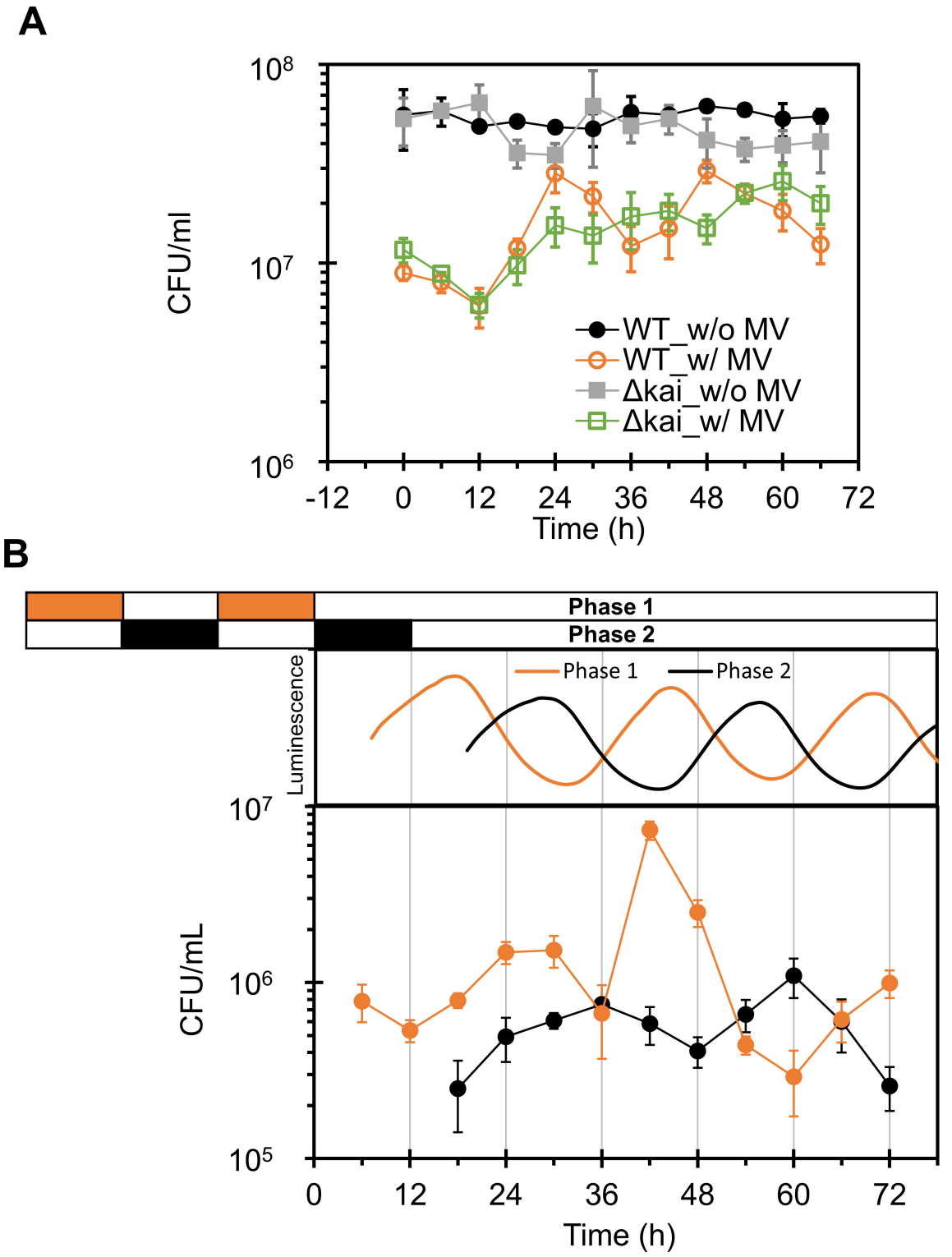
A
CFU/ml
10^8
10^7
10^6
-12
0
12
24
36
48
60
72
Time (h)
WT_w/o MV
WT_w/ MV
Δkai_w/o MV
Δkai_w/ MV
B
Phase 1
Phase 2
Luminescence
Phase 1
Phase 2
CFU/mL
10^7
10^6
10^5
0
12
24
36
48
60
72
Time (h)

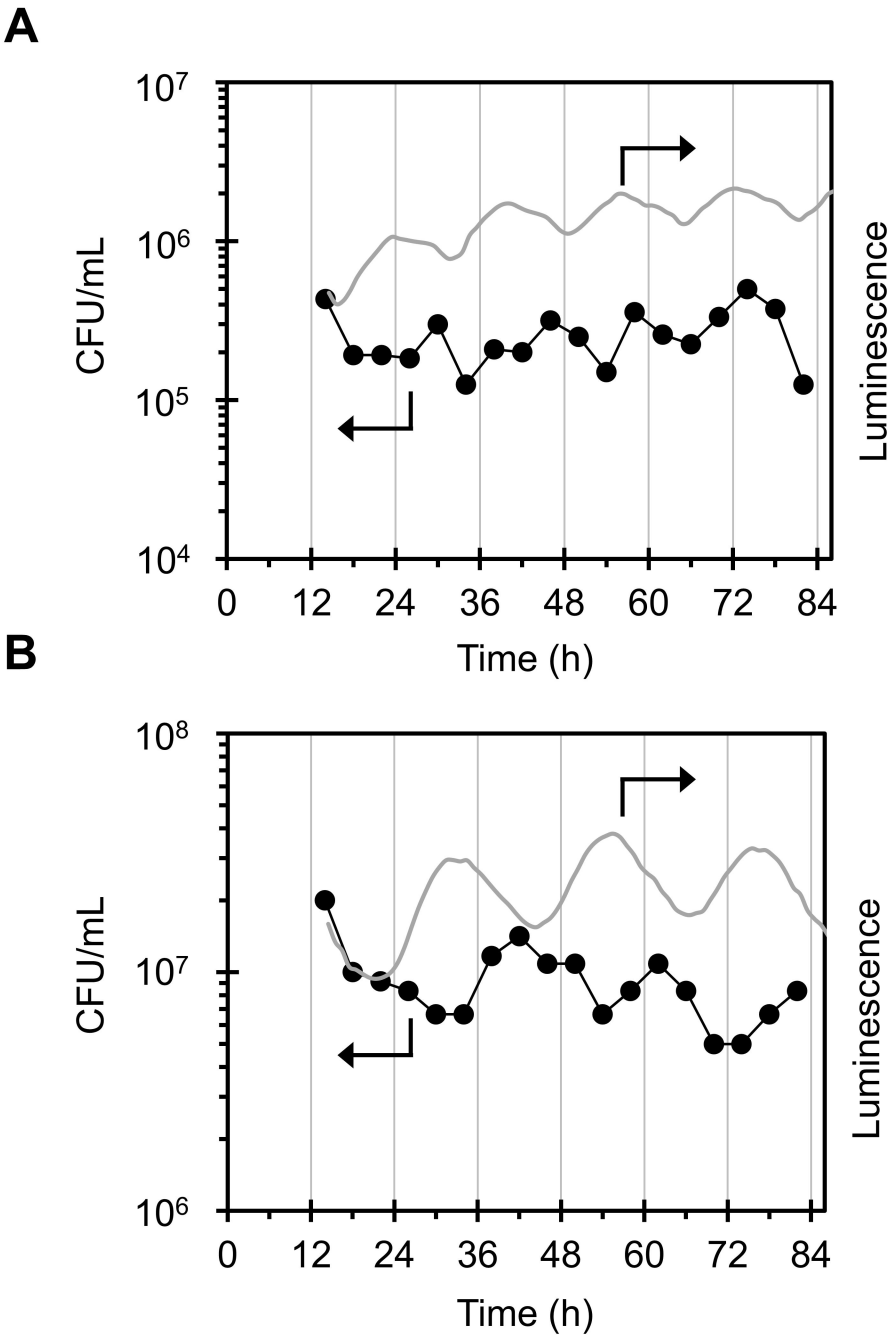
A
10^7
10^6
10^5
10^4
CFU/mL
Luminescence
0
12
24
36
48
60
72
84
Time (h)
B
10^8
10^7
10^6
CFU/mL
Luminescence
0
12
24
36
48
60
72
84
Time (h)

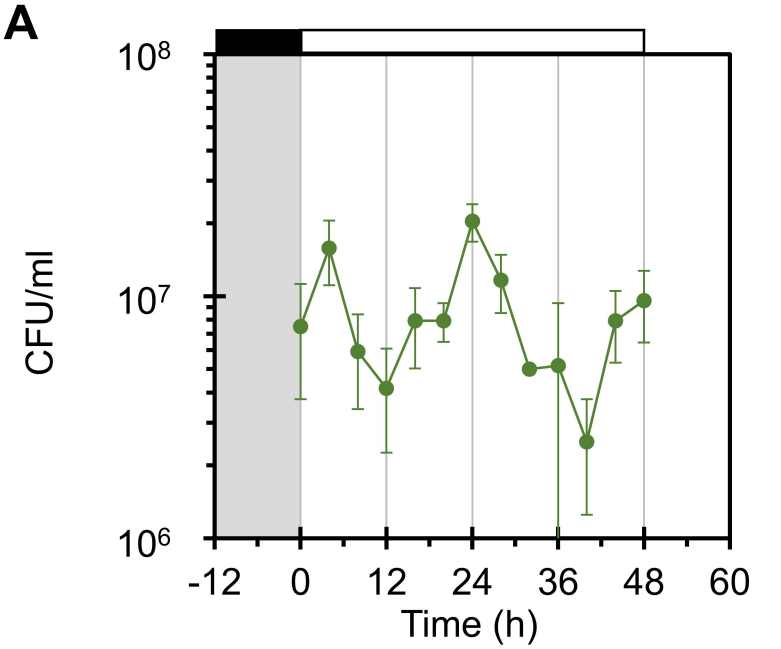
A
CFU/ml
10^8
10^7
10^6
-12
0
12
24
36
48
60
Time (h)

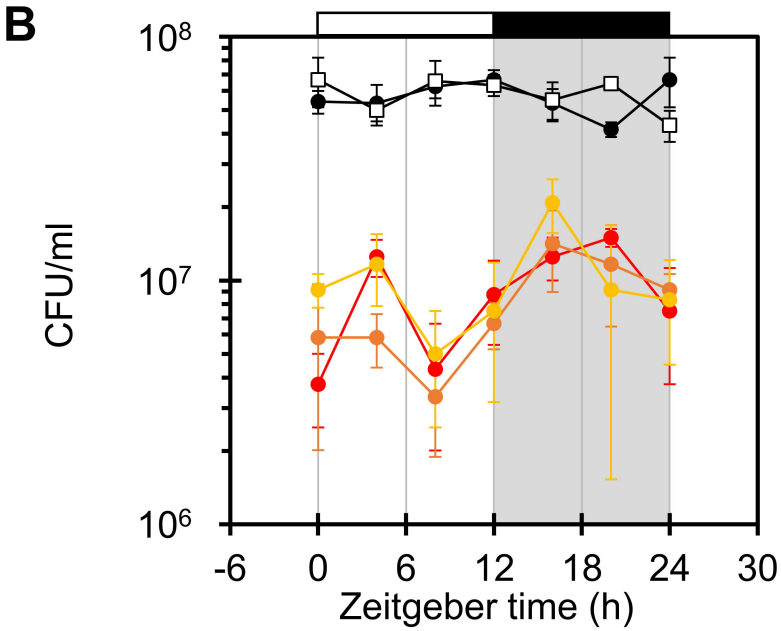
B
CFU/ml
10^8
10^7
10^6
-6
0
6
12
18
24
30
Zeitgeber time (h)

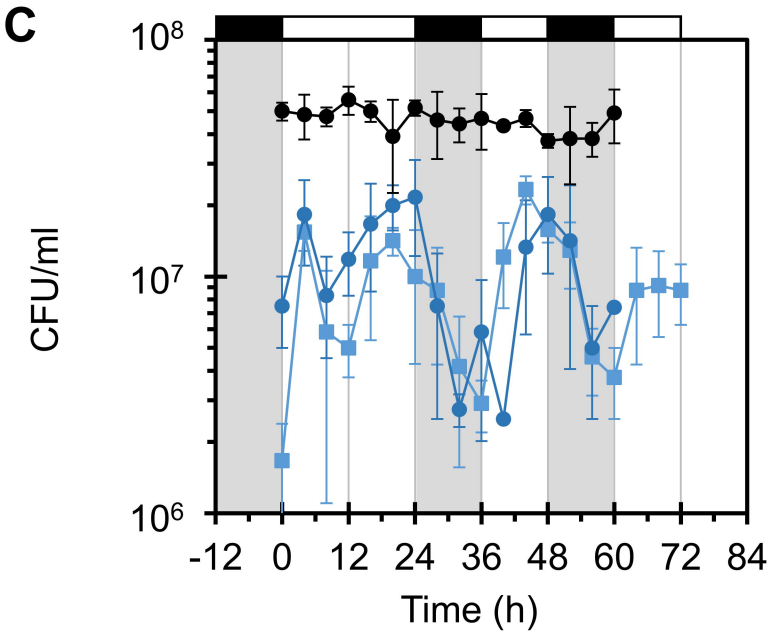
C
CFU/ml
10^8
10^7
10^6
-12
0
12
24
36
48
60
72
84
Time (h)